

# HyperXite Braking



**Adrian Francisco Duran Ornelas**  
aformela@uci.edu

- Design, Validate, and Assemble Twin HX VII Failsafe Braking Assembly
- Manufacture testing apparatus and programming of wireless GUI Interface

---

**Allen Hsing**  
hsinga@uci.edu

- Assemble and run tests on the braking test rig
- Assemble and test the pneumatics subsystem

---

**Elizabeth Chiu**  
chiuem@uci.edu

- Develop code and assemble the sensors circuit for the braking test rig
- Assemble and test the pneumatics subsystem

---

**Rahul Sheth**  
Rmsheth@uci.edu

- Design and develop a failsafe
- Create braking timeline
- Assist in validation of braking systems

MAE 189: Capstone Design  
Spring 2022  
University of California, Irvine  
Professor Roger Rangel  
6/10/2022

## Executive Summary

The Hyperloop pod is a vehicle that is set to revolutionize the technological advancement of transportation systems. Like the bullet train, it is meant to transverse from point A to B at a tremendous speed, making it convenient for people that rely on transportation systems for traveling and commuting. However, the Hyperloop pod is designed to travel through a vacuum tube to negate air friction so that the pod can achieve high accelerations. Ideally, the concept compensates the practical modes of transportation by being relatively inexpensive compared to airfares and fast compared to public transportation methods.

This year, HyperXite will be competing in European Hyperloop Week (EHW), a competition for Hyperloop teams to compete for awards for their Pod's mechanical, electrical, propulsion, and levitation systems, in addition to Pod completeness and scalability. However, beyond Pod performance, EHW has included a new Research Submission as part of the competition, designed to highlight Hyperloop-related research findings; this addition highlights EHW's desire to spotlight not only current technical achievements in the Hyperloop technology but also future potential developments.

Similarly, as a Senior Design Project as part of the Henry Samueli School of Engineering at UC Irvine, one of our major goals is to promote student learning through the work that we do, especially since our team includes students of different engineering disciplines, such as Mechanical, Aerospace, Electrical, and Computer Engineering. We encourage our members to explore designs and topics that interest them, allowing them to expand their knowledge in their personal areas of interest and discover potential new methodologies to improve our Pod.

For the past seven years, HyperXite has been working on the development of a small-scale hyperloop pod for the purpose of researching and developing the propulsion, braking, stabilization, and electronic systems aspects of Hyperloop. Our long-term objective is to align the development of our technology with the full-scale application of Hyperloop. To achieve this implementation goal, we account for conceptual and design considerations that would be important for the feasibility of high-speed, vacuum tunnel transportation, such as minimizing pod footprint to increase aerodynamics and efficiency. Other important considerations include maximizing the acceleration phase and minimizing braking distance to advance the Hyperloop's high-speed capabilities. Optimizing speed through current-to-power consumption and reducing latencies in our networking to enhance reliability. A recent effort on our team to achieve this goal is the development of a double-sided Linear Induction Motor for increasing thrust capabilities and decreasing friction losses.

Our goal to develop technology directly applicable to the Hyperloop concept is iterative in nature and is a result of prototype development, design analysis, and testing metrics. This year, our focus lies in utilizing testing data for a more informed and targeted design. Using data from last year, we have identified key aspects of our pod's design that can be strengthened. For this year's pod, we have set a loose requirement of a 4-foot long, 11-inch wide, and 9-inch tall pod with a mass of 80kg. With these requirements, we have moved forward with a dual motor design to double our speed, a pneumatically actuated friction braking system that reduces the overall braking distance by 33%, and a redesigned power system that modulates power consumption.

To meet these design requirements, we are working on a new motor selection process using an internally developed trajectory simulation and redesigned suspension geometries. The stabilization team utilized MATLAB's Simulink to develop a multi-degree of freedom pod model based on derived equations of motion to select the best stabilization parameters. In parallel, the research and development team is designing and prototyping a Linear Induction Motor that will reduce friction losses and allow for much higher acceleration and top speed. Coupled with a redesigned braking system that increases the pod's deceleration to upwards of 3G's, we anticipate a trajectory with a top speed of 35 m/s on a 100m track. Moreover, electronics is working to support the team's endeavors through integrating robust protective circuitry and designing high speed-signal PCBs verified through programs like ANSYS ICEPAK and SI WAVE. Power Systems is also creating models through MATLAB that allows the team to understand the characteristics of high voltage systems and pinpoint our optimal design for speed and reduced power consumption. In tangent, the controls team is developing reliable communication networks that display all the pod's parameters on a graphical user interphase (GUI). This interphase will allow us to read values from all our sensors and control the pod remotely. An additional goal this year is displaying a 3D model of the pod that demonstrates the position and speed.

Success on our team encapsulates more than building a Pod. By designing for EHW, our team strives to improve each Pod that is built in subsequent years, whether that is increasing the top speed and acceleration, increasing the PCB efficiency, decreasing the braking distance, or any other technical requirement. With throughout documentation of current work, we hope that future years of the HyperXite team and other Hyperloop organizations are able to use our developments to help drive the future of Hyperloop technology.

## Table of Contents

Executive Summary .....	2
List of Figures .....	6
List of Tables .....	7
Chapter 1: Problem Definition.....	8
Chapter 2: Conceptual/Preliminary Design (Design of Key Components) .....	9
Actuator.....	9
Gas Springs .....	10
Linear Rails.....	10
Brake Pad .....	11
Web Design.....	11
Flange Assembly Design .....	14
Fail Safe .....	16
Final Preliminary Design .....	17
Braking Test Rig.....	19
Chapter 3: Detailed/Critical Design.....	21
Detailed Engineering Analysis and Component Testing .....	21
Detailed Bill of Materials (BOM).....	22
Engineering Assembly Drawings .....	23
Prototype Plan.....	23
Identify methods for procuring parts and fabrication services .....	23
Define prototype build process .....	23
Document any tooling, jigs, materials, sketches.....	24
Define initial tests and expected results.....	25
Develop validation plan .....	26
Prototype Risk Assessment.....	27
Chapter 4: Prototype Performance and Final Design .....	27
Prototype Verification.....	27
Detail Test Conditions and Quantify Results.....	27
Compare results to initial performance requirements.....	27
Photos with Annotations .....	28

Description of Final Design .....	28
Document prototype development and redesign.....	28
Finalized Engineering drawings .....	29
Finalized Bill of Materials .....	30
Detailed Cost Analysis.....	33
Safety and Risk Assessment .....	34
Chapter 5: Design Recommendations and Conclusions .....	36
Acknowledgements.....	37
References.....	37
Appendix.....	38
Assembly Documentation.....	38

## List of Figures

Figure 1 - HyperXite VI Braking Assembly .....	8
Figure 2 - CAD Example of a Double Acting Pneumatic Cylinder .....	9
Figure 3 - CAD Drawing of pneumatic actuator used in the HyperXite VII Pod .....	9
Figure 4 - Gas Spring.....	10
Figure 5 - Linear Rails Schematic .....	11
Figure 6 - Visualization of Flange and Web of I-Beam.....	12
Figure 7 - Conceptual Sketch of forces in an angled actuating design.....	12
Figure 8 - First iteration of the web brake design featuring 15-degrees actuating angle.....	13
Figure 9 - Annotated perpendicular web design.....	14
Figure 10 - Four Actuator Flange Design Draft with Visualization of Keep-Out Zone.....	15
Figure 11 - Linear rail moment visualization .....	15
Figure 12 - Twin Carriage Actuator Flange Design .....	16
Figure 13 - Failsafe involving an electromechanically mechanism.....	16
Figure 14 - First design concept of a mechanical failsafe .....	17
Figure 15 - Final preliminary design of HX VII braking assembly.....	18
Figure 16 - Braking system under various dynamic loading conditions .....	19
Figure 17 - Braking Test Rig with Annotated Components and Mesh Removed .....	20
Figure 18 - Static study of pocketed braking base under maximum expected loading .....	22
Figure 19 - HXVII Finalized Design .....	23
Figure 20 - First 14 pages of Assembly Documentation .....	24
Figure 21 - Gas Spring Mount Drilling Jig 1 .....	25
Figure 22 - Pod After Assembly in Lab.....	29
Figure 23 - Pod on I-Beam During Pod Runs.....	29
Figure 24 - Final Engineering Drawing .....	30

## List of Tables

Table 1 - Interim Bill of Materials .....	22
Table 2 - Finalized Bill of Materials.....	33
Table 3 - FMEA .....	35

## Chapter 1: Problem Definition

The purpose of the braking system is to ensure a safe stop of the entire pod after it reaches its top speed. For this year's hyperloop we will be using a braking system based on pneumatically actuated friction brakes. Last year our target braking goal was to achieve a braking deceleration of 2G's. This year our goal is to maintain the minimum braking deceleration of 2G's or  $24.5 \text{ m/s}^2$  while simultaneously redesigning the system to be failsafe. To define our design requirements, we read the rules set forth by the European Hyperloop week. The primary criteria our braking system must meet is that the braking assembly must be able to safely decelerate the pod without causing damage to either the pod or track we are braking onto. Another design requirement is the fact that the braking system must minimally have two degrees of redundancy. This means that if the any system fails, including the brakes themselves, we must still have an avenue such that can stop the pod safely. One of our goals this year is to completely redesign the braking system to transition into a safer failsafe design. Below is an image of last year's braking system design.

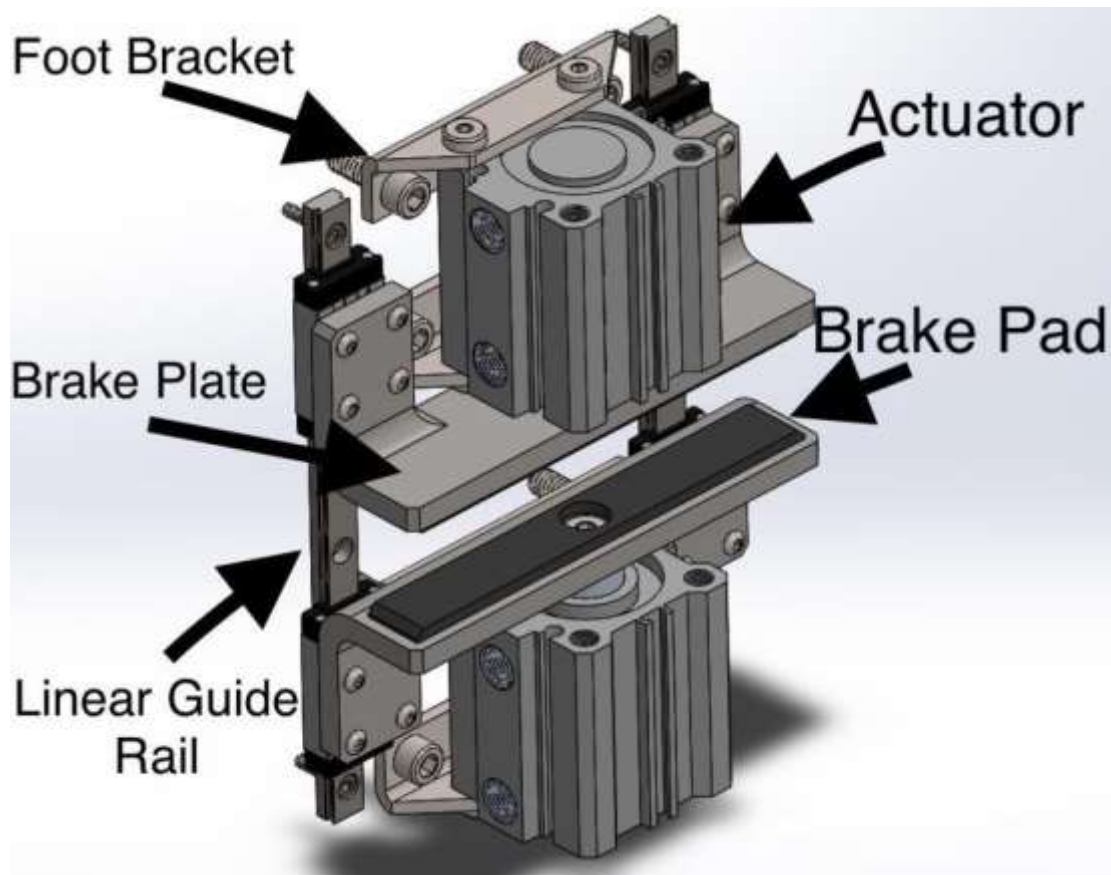


*Figure 1 - HyperXite VI Braking Assembly*

While this system was able to generate braking force that we built it for; there were problems with the design. One of the major problems was that the braking system would forcibly unmount when it would collide with an imperfection in the track. Additionally, this braking system fell short of the 2g's of braking force goal when operated with a factor of safety of two.



## Chapter 2: Conceptual/Preliminary Design (Design of Key Components)

### Actuator

An actuator is a piece of hardware in a device or machine that helps it to achieve mechanisms by converting electrical, pneumatic, or hydraulic energy to mechanical force. This includes rotary motion, such as a DC motor within a power drill, or linear motion, such as a pneumatic cylinder that will provide the braking force to the pod are all examples of how an actuator takes a non-mechanical energy and turns it to a mechanical force.

For the braking system employed in the HyperXite VI pod, a pneumatic cylinder actuator provides the force needed to apply the brakes onto the I-beam. Specifically, a double-acting pneumatic cylinder actuator was determined for the assembly for its ability to have controllable piston movements without relying on internal springs that are found in single-acting actuators that provides the opposing force to air pressure. Application of air pressure in a double-acting cylinder produces a thrust in the positive (push) stroke and thrust in the negative (pull) stroke.



Figure 2 - CAD Example of a Double Acting Pneumatic Cylinder

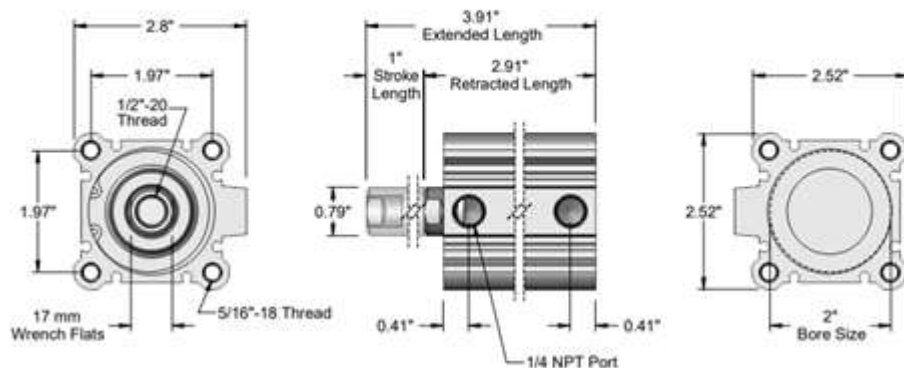


Figure 3 - CAD Drawing of pneumatic actuator used in the HyperXite VII Pod

Considering the pod's weight of 80 kg and a maximum speed of 35 m/s, the target braking force to reach 2 g's of braking deceleration needed is 1570N. The actuators in the HyperXite Pod VII serve a different purpose than in different years. Previously, the actuators would be the primary source of our braking deceleration, however with the introduction of our new failsafe design, they instead

restrict the application of our gas springs so that we can maintain braking force in the event of a pneumatic or electrical failure.

### Gas Springs

A gas spring is a type of spring that is similar to a traditional mechanical spring, but instead of relying on the elastic region of deformation of a material it relies on compressed gas inside a sliding piston to store potential energy instead.



*Figure 4 - Gas Spring*

In our braking design we are using a miniature gas spring in order to apply our braking force. By designing the braking system in this way, we are able to ensure that it is able to continue working in the event of a pneumatic failure. Through this way we have converted our dual acting pneumatic actuators (see above) to Fail-Close actuators. In this configuration the actuators serve to compress the gas spring, and effectively depress the brake pads from the track. Under normal operation we vent the actuators and allow the gas spring to extend onto the track in order to brake in a manner that resists failure conditions and ensures that we constantly will have the braking force we need.

### Linear Rails

Linear Rails are designed in order to facilitate the movement of an object with as little friction as possible while also restraining the motion exclusively along the axis of rail itself. Fundamentally the linear rail itself is a machined piece of steel that a carriage slides onto. This carriage is responsible for restraining motion in two dimensions and all three moment directions. Fundamentally it works as a carriage wraps around the dovetail pattern of a linear rail which only allows motion linearly along the axis, preventing all rotational movement and nearly all translational movement.

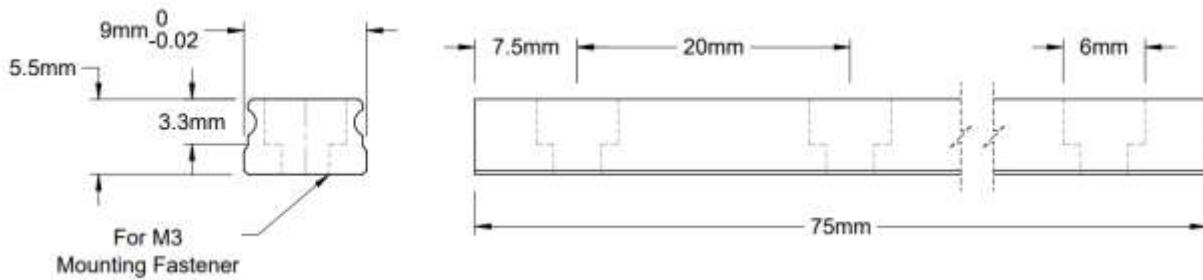


Figure 5 - Linear Rails Schematic

For this component, the flange braking design relies heavily on the ability for the linear rails to sustain yaw moment loads. During the application of the brake pad onto the I-Beam, the force of friction equals an opposite force onto the braking subassembly itself. In order to withstand the large moment created without damaging the stroke arm of our pneumatic actuator we need to incorporate the use of linear rails to restrict the possible movement.

### Brake Pad

The brake pad is the part of the braking system that contacts the I-beam and is made of Bremskrel 6061. The purpose of the brake pad is to generate the friction of the braking system. The material will wear evenly as it rubs against the track. The brake pad will be held to the braking system by an industrial epoxy adhesive. One of the main requirements for this part of the braking system is that it must not damage the track while it rubs against the track. The softness of this material is softer than the hardness of the track, and we are validating this experimentally through our pod runs. In addition, to increase the effectiveness of the initial application of braking force this year we are introducing a chamfer on the braking material in order to better be able to endure imperfections in the track surface.

### Web Design

The brakes are able to engage onto the flange or the web, see figure below. During a review of last year's braking design, it was discussed that the flange brakes have the potential to collide with the I-beam if they happened to be misaligned. Specifically, one I-beam would be mounted so that it is higher than the consecutive beam. It was considered that braking on the web would mitigate the issue as misalignment would be either minimal or nonexistent on this area of the I-beam.

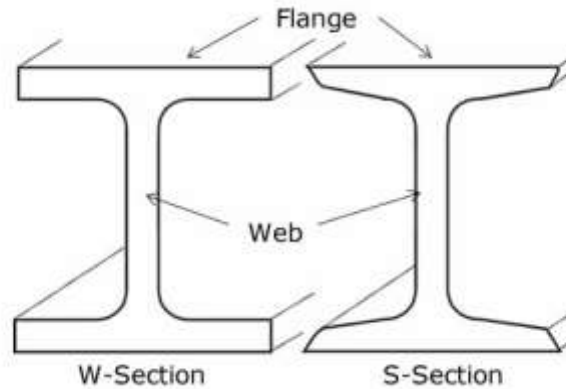


Figure 6 - Visualization of Flange and Web of I-Beam

One of the initial challenges when designing the web brakes was to fit the braking assembly within the tight constraints of the chassis. It was determined to have the brakes engage on an angle with the drawback of having less braking force to the I-beam for the first initial iterations of the braking design. The braking force will be directly proportional to the angle of actuation as it breaks the actuated force to an x and y-component (see Figure 7).

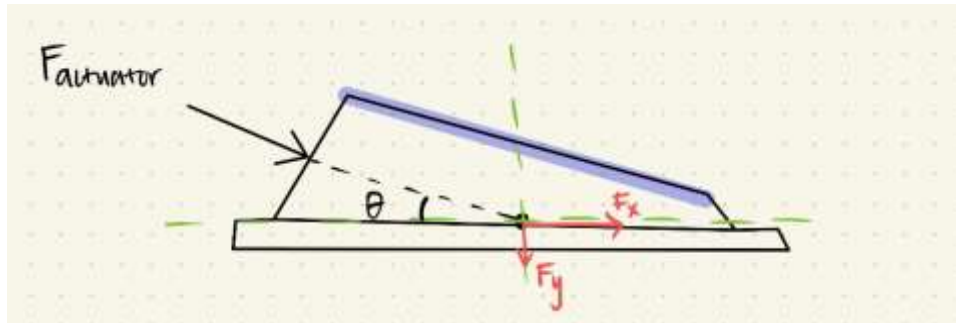
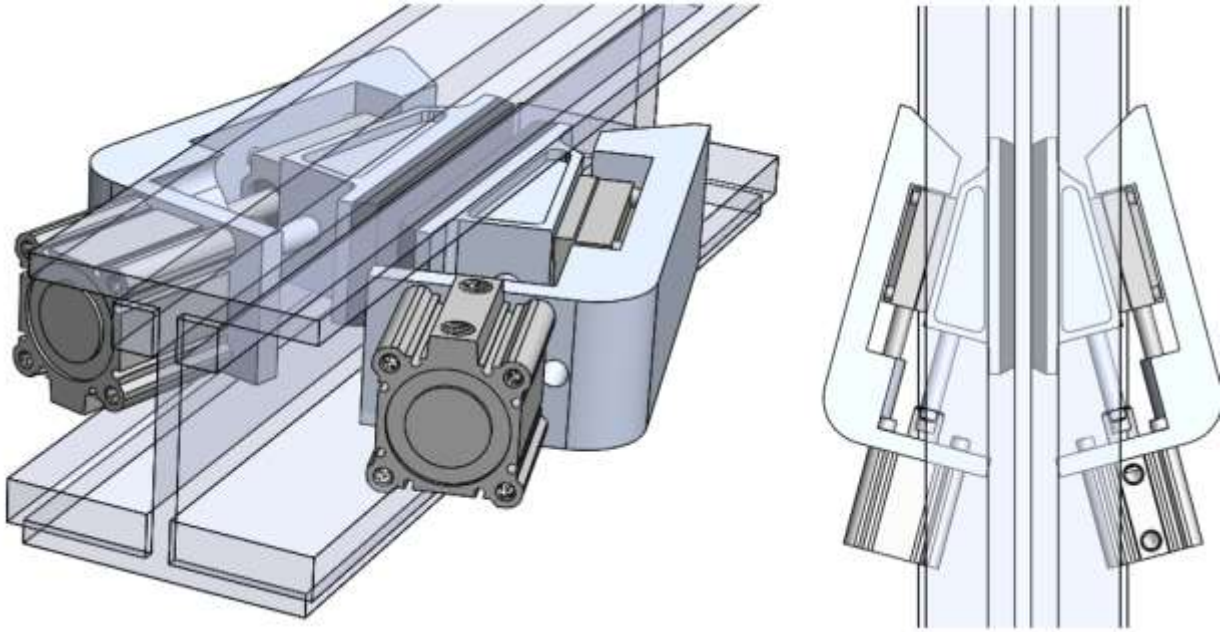


Figure 7 - Conceptual Sketch of forces in an angled actuating design

The initial CAD model of the web braking design was angled to 15-degrees from the I-beam (see Figure 7) to minimize horizontal real-estate within the chassis from the I-beam. This model limited horizontal width at 10.3 inches including the intended mounts. Since the braking force from the pneumatic cylinder is directly proportional to the angle of actuation, using an actuator that can provide a total of 456lbf at 145psi meant the total normal force was only 118 lbf. To put into perspective, for the pod to decelerate at 3.0G within one meter, the actuator must supply about 265 lbf which is impossible for this actuator and angle.



*Figure 8 - First iteration of the web brake design featuring 15-degree actuating angle*

Upon further investigation, the web design was iterated to fully utilize the actuator force while maintaining a small profile relative to the space within the pod. The latest web design was considered with a simplistic approach while maintaining a conservative budget. This design actuates normal to the I-beam employing a heavy-duty actuator capable of supplying up to 410 lbf. This force translates to 192.7 lbf of frictional force, which is resisted by two colinear stainless steel rods mounted lateral to the actuator each withstanding up to 160,000 psi. To ensure smooth and safe actuation, the rods are guided by heavy-duty linear bearings that will be press-fitted into the machined aluminum housing. The linear bearings are rated to resist loads up to 590 lbf resulting to a factor of safety of 3. A pair of this braking assembly theoretically provides the whole pod 2.2G of deceleration with a width of about 4.25” on either side of the I-beam.

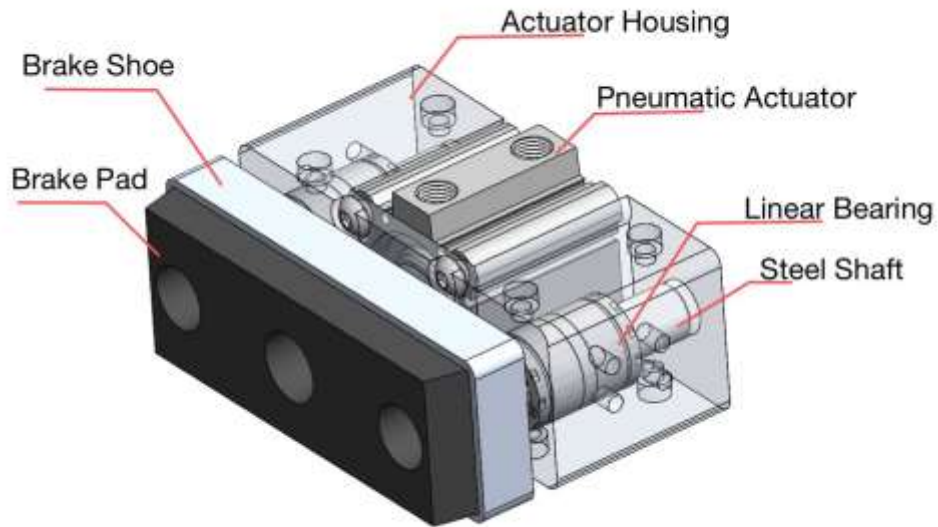


*Figure 9 - Annotated perpendicular web design*

Compared to the early iteration of the web design, the new design's simplicity allows for less complex mounting and manufacturing reducing the cost to machine the aluminum housing and brake pad mounts. The design features mounting holes on either side of each unit and on the top and bottom face for mounting versatility. Overall, the cost of the hardware for this design is minimized but is off-set by the cost of manufacturing both the actuator mount and the braking shoe. The cost of manufacturing can be substantially decreased if parts are manufactured in-house using either a 3-axis CNC or CNC mill.

### **Flange Assembly Design**

Last year on the Pod VI, the flange design consisted of four 62245K182 actuators firing at once onto the flange of the I-Beam, providing a net braking force of 1094 Newtons. This year's flange design was designed explicitly to improve upon the previous year's design while prioritizing the reuse of old hardware to save money. In order to more easily clear track imperfections each braking assembly will be independently mounted to the pod track with a greater clearance from the I-Beam to increase both the ability to both clear imperfections and in the event of a collision to avoid having the braking assembly shear off.

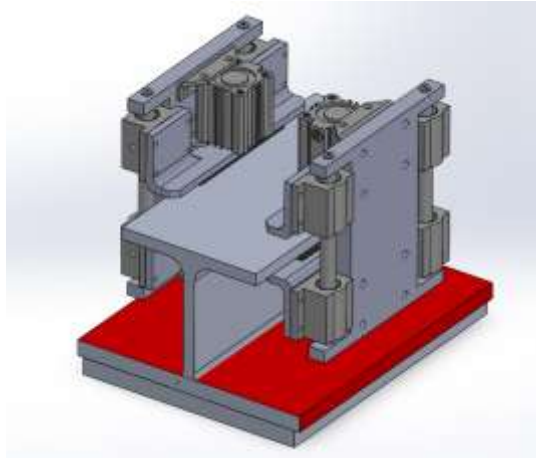
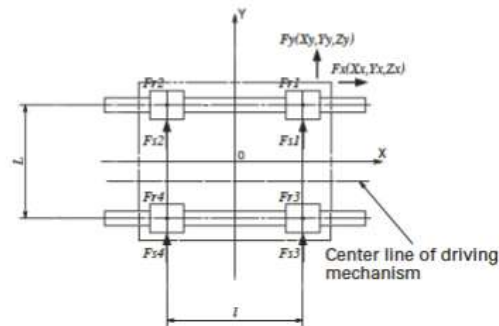


Figure 10 - Four Actuator Flange Design Draft with Visualization of Keep-Out Zone

The first iteration of our CAD model for the flange design consisted of a placeholder actuator and four linear rail carriage per actuator stabilization system. While this design could withstand the great shearing moment of the reaction force to the friction because of the large mechanical advantage, it was very expensive and was not close to an optimized design. Some of the major design considerations that went into this design was the two-by-two parallel linear rail carriage array shown in Figure 11.



When dual guide rails with two bearings each are used, only downward ( $F_r$ ) and side ( $F_s$ ) forces are induced; no pitch, roll, or yaw moments.

Figure 11 - Linear rail moment visualization

While this offered a complete elimination of the yaw moment that we need to resist, it comes at the price of doubling the amount of money we need to spend on carriages in order to safely sustain the yaw moment. Therefore, going forward we elected to only use two carriages per braking actuator as opposed to four. In Figure 12, an early draft of the HX VII braking system is present and is characterized by its twin carriage actuator design. Through this configuration, it was possible to double the effective force applied by the previous year's braking system, in addition to operating with a higher factor of safety because of the increase in moment resistance offered by the improved SEL2BZ16 linear rails.



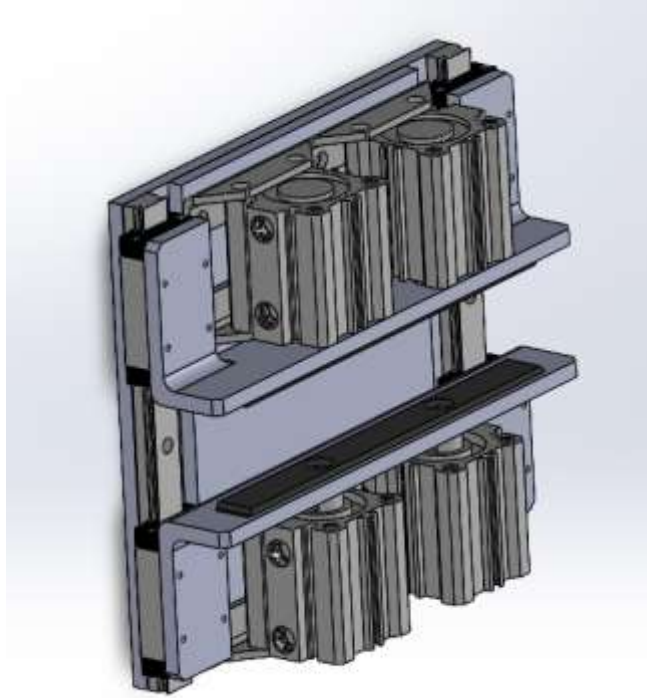


*Figure 12 - Twin Carriage Actuator Flange Design*

### Fail Safe

Below is an example of our first idea of a fail safe for the braking system. The drafted system works based on an electromagnetic force. The electromagnetic force holds a mechanical spring in place such that when the power is cut off the electromagnet no longer generates a magnetic field and the spring is released which allows the brake pad to contact the surface.



*Figure 13 - Failsafe involving an electromechanically mechanism*

After investigating this design and doing some hand calculations, we found that the magnetic field needed to generate a strong enough force to hold the spring in place was greater than 500 watts of continuous load. This value was too high for safe operation off the batteries we were implementing so we decided to move to a mechanical design that did not rely on electromagnetic forces.



Below is a picture of our first design concept of a mechanical failsafe. The working principle is that the failsafe will be held by two latches that will compress a spring. The latches will release when a motor pushes the latch laterally and the spring will release to generate braking force.

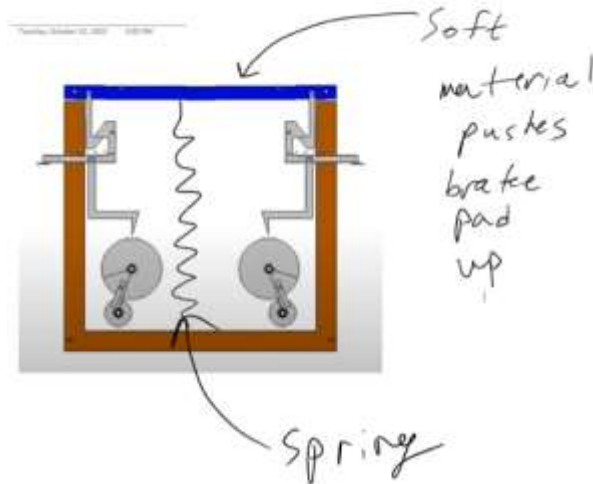
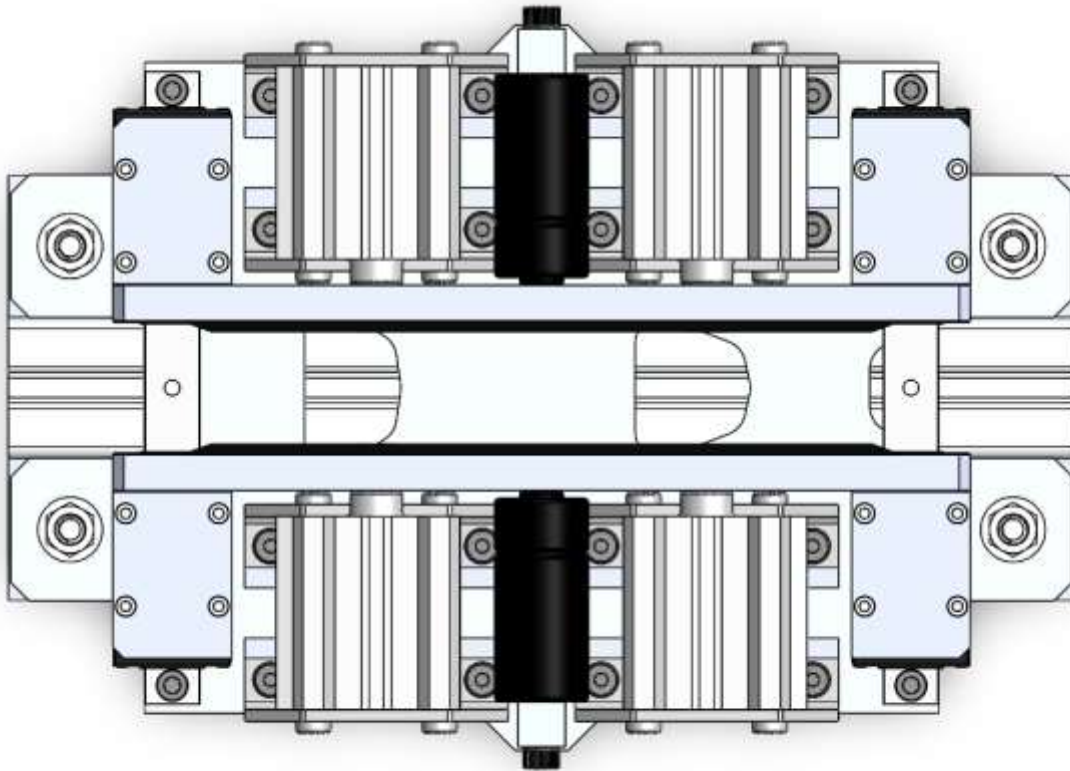


Figure 14 - First design concept of a mechanical failsafe

After computing the forces on the design, we found the required force to push the latches is greater than 25 lbf. While by optimizing we were able to minimize the actuation force to release the spring far lower than the about of force stored in the spring, we were unable to find an effective manner of actuating the design as servo motors in the size that the design required were not powerful enough. A discussion of the final fail-safe mechanism is continued in the following section.

### Final Preliminary Design

Previously, we were designing two independent systems, the traditional friction based pneumatically actuated system that we had already had experience creating in addition to a separate fail safe model. Going forward we consolidated fail safe and pneumatically actuated flange braking design into a singular failsafe design. This combination resulted in a fail-safe braking system that is able to maintain braking force even in the event of a pneumatic or electronic failure. The biggest departure from Pod VI's braking system is the shift from being pneumatically actuated to pneumatically constrained.



*Figure 15 - Final preliminary design of HX VII braking assembly*

While the working principle in the fail-safe pneumatically constrained braking system remains the same, with the difference being the source of the braking force. Pod VII features a miniature gas spring on all four brake pads that provide a 770 Newton force directly onto the track for a net force of 3080 Newtons. The gas spring is held in a compressed state by the 62245K182 pneumatic actuators. Under a braking load, the force of braking is transferred through the linear rails to the rest of the pod with the loading shown in the following image. With the introduction of the gas spring to the bracket analysis, Pod VII's design was made to be stronger in order to avoid plastic deformation during braking while using lighter 5052 Aluminum.

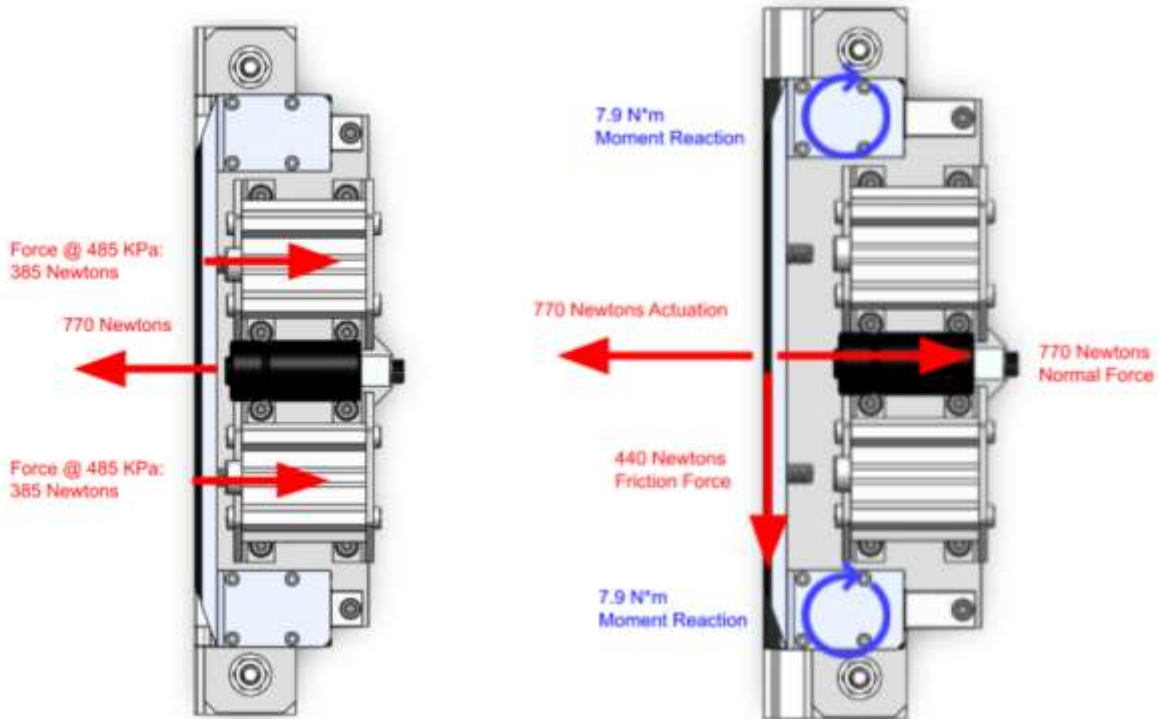


Figure 16 - Braking system under various dynamic loading conditions

Our braking pneumatic constraint system is operating as an Air-to-Open Fail-Closed reverse acting actuator, as the pneumatic actuators serve to hold the gas spring back. By taking the failure modes of the braking system into consideration, we have determined that a reverse acting actuator is the best implementation for the braking system to minimize cost while maximizing the overall safety and stopping capability of the Pod VII braking system. The dimensions of the design was dictated by the vertical height constraints of our mounting position on our pod. One of our design goals when determining the relative positions of the components was maximizing the vertical distance of our brake pads, to the surfaces of the I-Beam. We were not constrained in the direction of motion, and therefore took advantage of our additional width in order to specify multiple actuators and therefore increase total braking force for the pod.

### Braking Test Rig

In order to test and validate our braking subsystem, we have devised a flywheel-based mechanism in order to collect experimental data from a scenario similar to real world braking. While collecting data on a braking system that functions on resisting a translation movement is hard for large initial velocities such as the 35 m/s we are targeting, we were able to get around this issue by employing a fly wheel. At the point of contact, the fly wheel surface moves tangentially at a speed of 35 m/s similarly to how the track would during runtime. Through this we are able to experimentally observe the amount of time it takes to decelerate the fly wheel to a stop, and through a physical analysis determine the real-world braking force that our design was able to apply.

Additionally, we are hoping to be able to utilize this testing apparatus for future years and as such we are working to ensure it is modular and easy to understand for future braking systems.

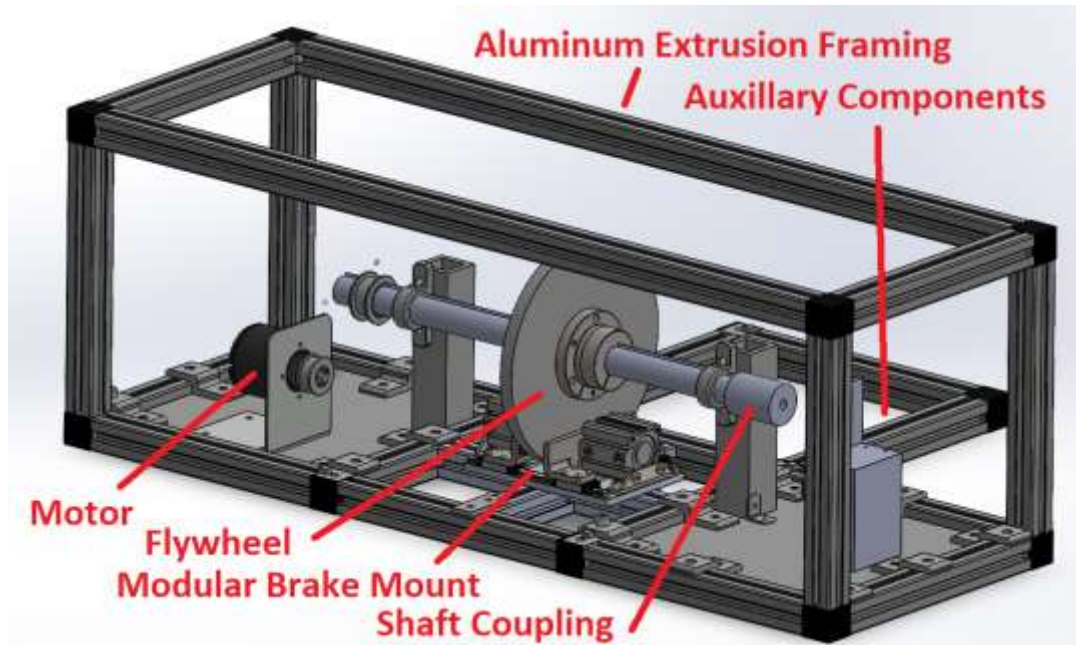


Figure 17 - Braking Test Rig with Annotated Components and Mesh Removed

In order to ensure the safety of team member when in the vicinity of the fly wheel we are taking several steps to reduce the dangers. Our first safety mechanism is physical distance. The braking test rig is meant to be operated at a distance of 15 feet away and can be operated completely wirelessly at distances within 30 feet. In the event that the braking test rig enters an unsafe state, such as loss of control or a physical failure, the safest way to approach it is to disconnect the power input remotely and for the fly wheel to come to a stop slowly. In the event of a physical failure, the steel mesh surrounding all sides of the test rig is meant to absorb as much of the impact as possible such that a fly wheel projectile has the majority its kinetic energy removed during the impact.

After confirming that the pistons travel at the same speed, we will integrate the actuator into the braking test rig and collect data on braking force, braking time, friction coefficient at our top speed, as well as monitor how this data is impacted based on temperature of the brake pad due to the thermal energy generated from contacting the aluminum surface. We will run several trials increasing the velocity each time to see how the friction force is affected. Based on these two tests we will be able to determine the kinetic coefficient of friction. The next test we run will determine how the temperature of the brake pad material affects the braking force and coefficient of friction. First we will run a Cold performance test (when the brakes have not been engaged for a long time and are cold) and a fade test (the reduction in stopping power after the repeated or sustained

braking applications). Using a thermal sensor, we will be able to track the temperature of the brake pad material and confirm that thermal energy dissipation will not be an issue for our system.

The final stage of testing on the full pod will be used to confirm our results from the braking test rig and ensure the braking system can stop the pod safely and effectively. In addition, we plan to confirm that the braking system can clear track misalignments.

## Chapter 3: Detailed/Critical Design

### Detailed Engineering Analysis and Component Testing

The braking system is manufactured as two twin assemblies mounted on both sides of the aluminum I-Beam flange (See Figure 6). We are outsourcing the majority of our steel manufacturing; for the gas spring mounts, we are additionally modifying the outsourced part in order to allow for tighter integration to our specific design needs.

For the braking system, SolidWorks Simulation and ANSYS Mechanical FEA platforms were used to validate the operational capacity of custom machined parts. We did not perform a finite element analysis on off-the-shelf parts and instead relied on the manufacturer specifications. The L-Bracket, made from 4130 Chromoly Steel with yield stress of 430 MPa, was determined to be one of the main points of failure because of the resistive load from actuation. However, during the static resting load it is under 80 MPa Von-Mises Stress located at the actuator mounting holes and corners, resulting in a factor of safety of 2.3.

#### **Image Pending Render – Static Loading Case**

#### **Image Pending Render – Dynamic Loading Case**

Our gas spring mounts are also made out of 5052 Aluminum. The forces can be seen in our SolidWorks analysis in Figure 3. This part undergoes a maximum Von-Mises stress of 85 MPa, localized at the edges of our support material. This part features a factor of safety of 2.1 and is projected to not fail under our maximum loading scenario.

#### **Image Pending Render – Gas Spring FEA**

We performed a Finite Element Analysis in Solid Works for the Braking Base Plate along with a Topology Study in order to minimize the weight of the braking system. The base plate is machined out of 6061 T6 Pocketed Aluminum.



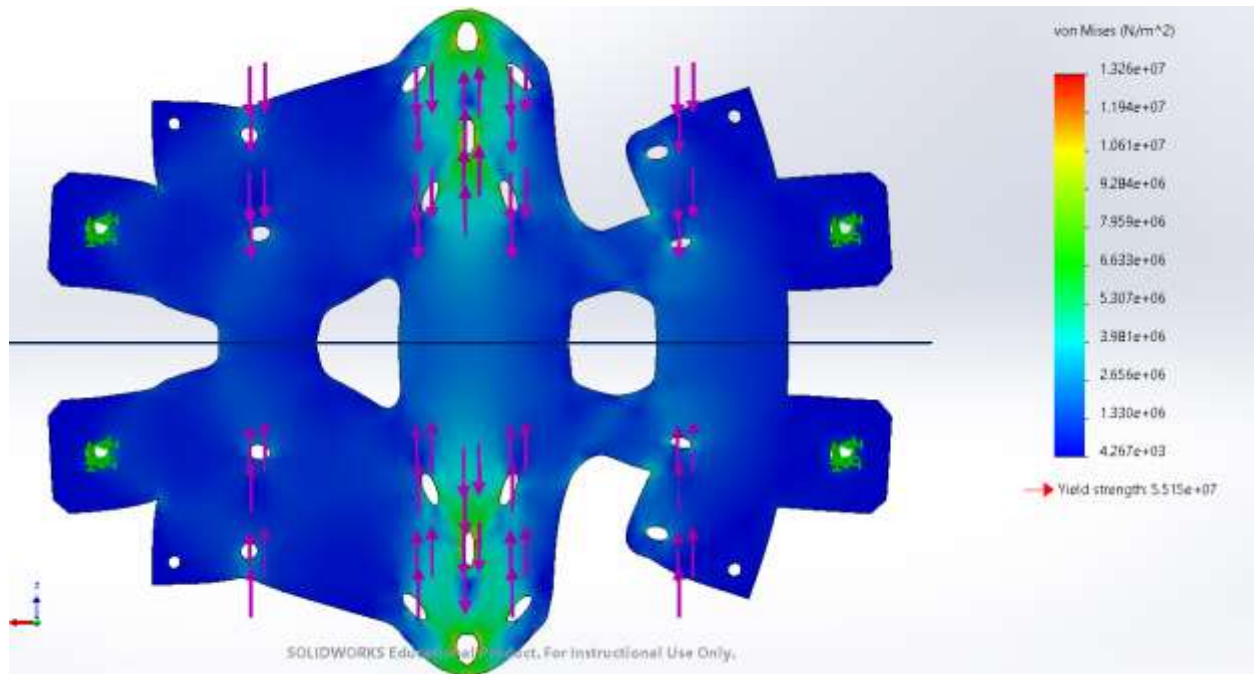


Figure 18 - Static study of pocketed braking base under maximum expected loading

## Detailed Bill of Materials (BOM)

Table 1 - Interim Bill of Materials

ITEM NO.	PART NUMBER	DESCRIPTION	QTY USED Per Braking System	QTY TOTAL	Orders to Place	Amount per Order	Price	Exhaustive Price	Need to Order	Supplier
1	99904A101	Medium-Strength Steel Serrated Flange Locknut	16	32	1	100	\$6.90	\$6.90	\$6.90	McMaster-Carr
2	92220A186	Alloy Steel Low-Profile Socket Head Screw	16	32	1	50	\$11.84	\$11.84	\$11.84	McMaster-Carr
3	91290A248	Black-Oxide Alloy Steel Socket Head Screw	8	16	1	50	\$11.08	\$11.08	\$11.08	McMaster-Carr
4	96194A202	Medium-Strength Steel Serrated Flange Locknut	8	16	1	100	\$8.88	\$8.88	\$8.88	McMaster-Carr
5	91290A321	Black-Oxide Alloy Steel Socket Head Screw	2	4	1	100	\$15.14	\$15.14	\$15.14	McMaster-Carr
6	92220A183	Alloy Steel Low-Profile Socket Head Screw	16	32	0	50	\$11.85	\$0.00	\$0.00	McMaster-Carr
7	92220A231	Alloy Steel Low-Profile Socket Head Screw	4	8	1	5	\$6.65	\$6.65	\$6.65	McMaster-Carr
8	62245K98	Foot Bracket for 1-1/4" Air Cylinder	8	16	16	1	\$8.07	\$129.12	\$129.12	McMaster-Carr
9	62245K182	Flexible-Mount Air Cylinder	4	8	8	1	\$61.68	\$493.28	\$493.28	McMaster-Carr
10	91290A115	Black-Oxide Alloy Steel Socket Head Screw	16	32	1	100	\$9.08	\$9.08	\$9.08	McMaster-Carr
11	11515t5	1.5" x 1.5" ALUMINUM EXTRUSION -11.5 inches	1	2	2	1	\$6.58	\$13.16	\$13.16	parco-inc
12	653185	CG322H Corner Gusset	4	8	8	1	\$6.10	\$48.80	\$48.80	framingtech
13	99904A102	Medium-Strength Steel Serrated Flange Locknut	8	12	1	100	\$10.34	\$10.34	\$10.34	McMaster-Carr
14	90044A425	Black-Oxide Alloy Steel Socket Head Screw	2	4	1	10	\$12.83	\$12.83	\$12.83	McMaster-Carr
15	93615A453	18-8 Stainless Steel Low-Profile Socket Head Screw	4	8	2	5	\$5.24	\$10.48	\$10.48	McMaster-Carr
16	55E12E216	High Strength Linear Rail + 2 Carriages	2	4	4	1	\$127.66	\$510.64	\$510.64	Mitsumi
17	8643K621	High-Force Miniature Gas Spring	2	4	4	1	\$8.89	\$354.76	\$354.76	McMaster-Carr
									<b>\$1,652.94</b>	

# Engineering Assembly Drawings

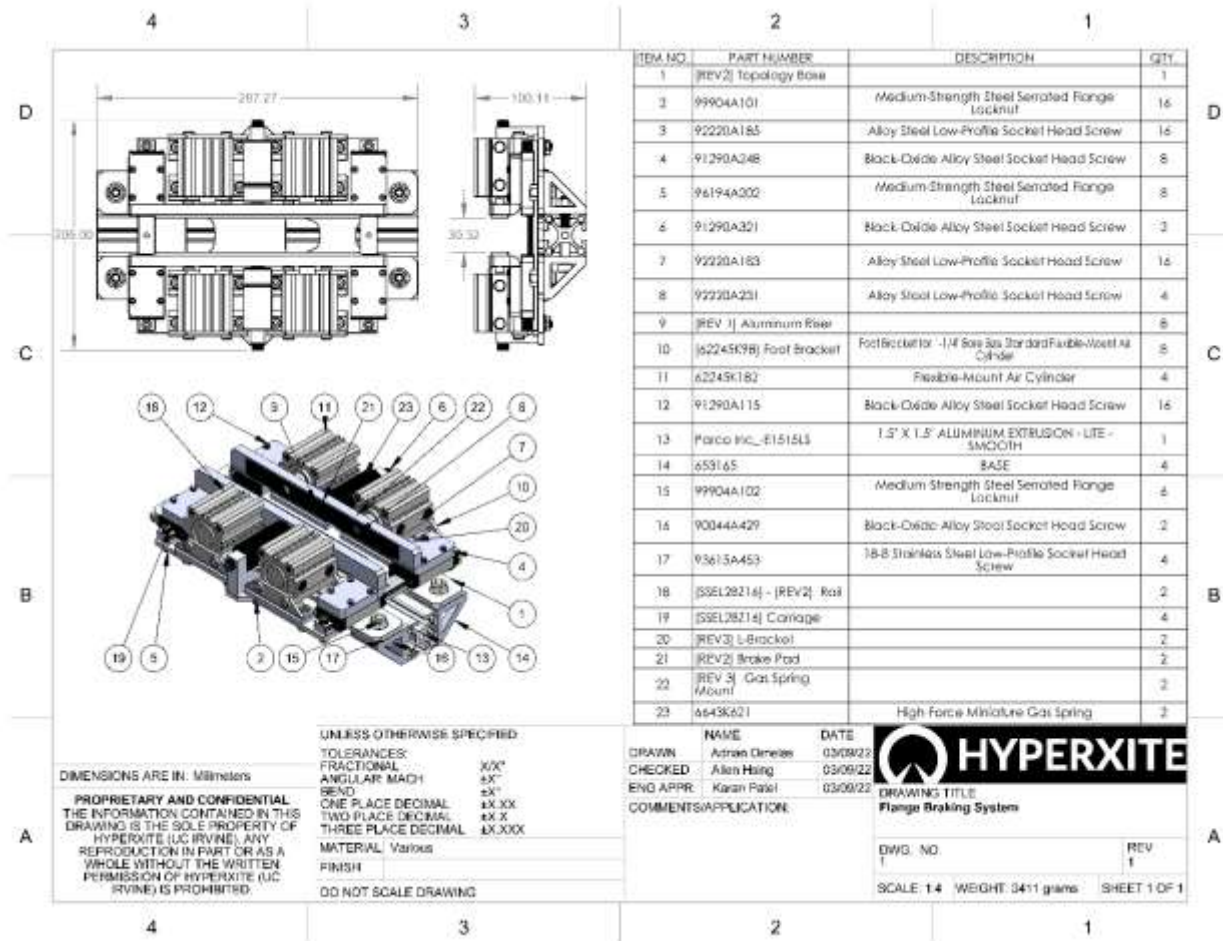


Figure 19 - HXVII Finalized Design

## Prototype Plan

Identify methods for procuring parts and fabrication services

We submitted quotes for various third-party fabrication services such as ATPrecision, Protolabs, and others. However, the most cost effective option for us is to machine the majority of our pieces at SendCutSend. SendCutSend is taking care of all of our manufacturing except for the gas spring mount. The gas spring mount is machined partly by SendCutSend, and then finalized by us with our own custom drilling jigs.

Define prototype build process

The Prototype build process is documented in our Braking Assembly documentation and is an exhaustive guide to the assembly of the braking system down to every fastener. The guide is styled in 14pt font and designed to be easily read and referenced during the assembly of the braking system. In Figure 20, the first 14 pages of the stylized assembly documentation to showcase the

readability of assembly instructions which is optimized for viewing on smaller devices to assist in manufacturing.



*Figure 20 - First 14 pages of Assembly Documentation*

Document any tooling, jigs, materials, sketches

While the majority of our machining is being outsourced to SendCutSend we still have to create specific contours they were unable to provide us with. In order to create these, we created drilling jigs in order to align the contours we need to drill to millimeter precision on our drill press. These Drilling jigs are created using additive manufacturing on a 3D printer and result in a sturdy part that will be able to withstand the torques associated with the drill. The jig is designed to be interchangeable in order to address the excess heat deforming the mounting solution. In addition to this the Jigs can be swapped out in order to reach different holes and contours and have proved successful when used in conjunction with the lab drill press.



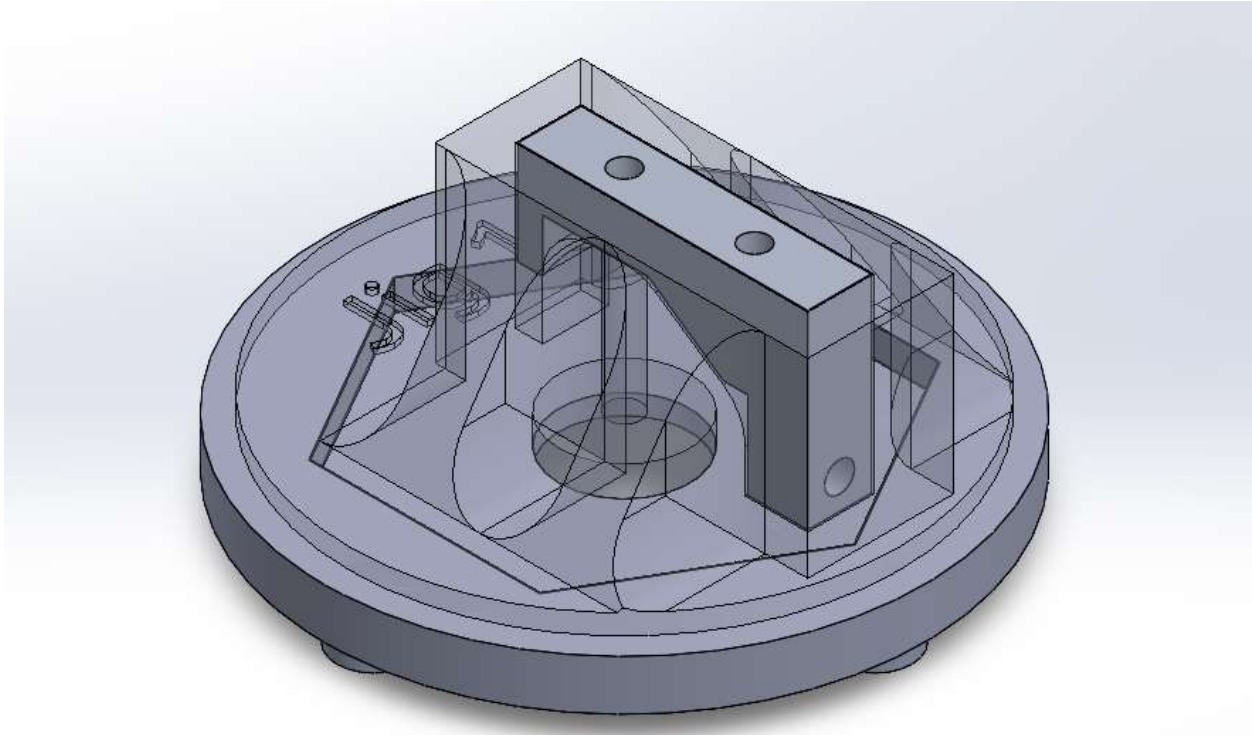


*Figure 21 - Gas Spring Mount Drilling Jig 1*

#### Define initial tests and expected results

In our first phase of testing, we plan to feed different pressures into the actuator to see how the pistons extend and retract. We will pay special attention to see if the pistons travel at the same speed and measure the time it takes for each piston to reach the middle point. For a CAD representation of the braking test rig see Figure 17. The braking system is tested in three phases: basic actuation testing, flywheel testing, and lastly full pod runs.

Actuation testing consists of recording multiple actuations to record the average time of actuation for each piston to reach the fully extended position. The goals of this test are to gauge whether or not we can assume the actuators fire and apply their braking force simultaneously and to validate the basic structural integrity of the brakes.

The next test consists of testing inside our braking test rig in where we record high speed video in order to derive the number of frames in 480fps video it takes to fully stop the flywheel at varying speeds. From this data we are going to apply a force inertia balance to calculate the average braking force from the deceleration of the rotating flywheel and shaft combination when introduced to the frictional braking force. The testing procedure is as follows:

#### *Braking test rig testing (Design Verification)*

**Objective:** To find the true coefficient of friction

1. Rotate the fly wheel equal to the max speed of the pod

2. Using the rotary encoder ensure the max speed is reached
3. Once the max speed is reached shut off the motor
4. Engage the brakes and measure the number of rotations required to bring the wheel to rest
5. Using the equation  $(\frac{1}{2})(I)(w)^2=(\mu)*(N)*(d)$  and solve for  $\mu$
6. Repeat for 10 trials and take the average to find the true coefficient of friction
7. Wait for 30 minutes in between trials to ensure that the brake pads are fully cooled to ensure that temperature doesn't affect the friction coefficient

**Objective:** Determine if Brake Pad temperature affects brake force

1. Measure brake pad thickness at  $N=0$
2. Repeat above testing without 30-minute breaks in between and see how the friction coefficient changes over the trials
3. We will track the temperature of the brake pad material using the thermal IR sensor
4. Measure brake pad thickness at  $N=10$

#### Develop validation plan

The final stage of testing on the full pod will be used to confirm our results from the braking test rig and ensure the braking system can stop the pod safely and effectively. In addition, we plan to confirm that the braking system can clear track misalignments. After determining that the braking system can adequately meet all of its stated requirements in the test rig we will shift towards beginning testing it in the context of the full pod during pod runs on our aluminum test track. We will then be documenting all of the experimentally obtained criteria we collect in our design documentation to be able to present during the European Hyperloop Week competition.

The testing procedure for Full Pod Runs is as follows:

#### *Full Pod Testing: (Design Validation)*

1. Measure biggest bumps in track misalignments
  - a. Use Calipers and pay special attention to areas in between extrusions
  - b. Note especially big misalignments
2. Do a pod run  $N=10$
3. Observe calculated braking distance and real braking distance from controls
  - a. Compare to the values found in the braking test rig and theoretical values
4. Observe brake pad wear
  - a. Using calipers measure brake pad material before and after runs
5. Observe system integration does the braking assembly withstand the forces exerted on it?
  - a. Look for any signs of the braking system moving while actuating
6. Does the braking system stay out of the No-Go-Zone

## Prototype Risk Assessment

The biggest risk for our prototype plan not being completed is not getting our components on time. We will track the components and if we notice that one of the components will not arrive before the start of next quarter, we will start researching for alternatives that could arrive faster. By designing in this way we have been able to maximize the amount of work we've been able to complete in the short 10 week quarters at UC Irvine.

## Chapter 4: Prototype Performance and Final Design

### Prototype Verification

#### Detail Test Conditions and Quantify Results

The Braking System for HyperXite VII was fully assembled in late May 2022, and its performance exceeded expectations. The majority of our testing was done on the HyperXite VI braking system due to an externality that was out of our control. However, the data that we collected was still insightful. By using the impulsive kinematic equations for a rotating body and applying the deceleration of the brakes actuated normal to the outside of the circle, we are able to derive the original braking force. Unfortunately for us, the braking system over preforms, and stops the rotating flywheel of the braking test rig instantaneously, and we were unable to get a hold of a camera that was capable of consistently recording above 960 frames per second. Through the near instantaneous actuation of the test we are able to estimate the braking force as above 500 Newtons, a low number relative to our projected amount limited by the time resolution of our camera and the low inertial mass of our flywheel.

Our secondary level of testing involves the actuation of the HyperXite VII braking system during the running of the pod. Again, unfortunately, the pod was unable to propel it self autonomously, so instead we reached a peak speed of three meters per second by propelling it manually. However, before we were able to actuate the brakes, a piece of our suspension began interfering with the track and prevented us from running the pod further. Because of this, we shifted to a more archaic method to test our braking system. Once clearing the interference with the track, we engaged the brakes, and 5 team members went to push the pod with as much force as they could. Given NASA's performance metrics for human performance, a rough estimate of the pushing power of a human is 262 Newtons, multiplied by five people results in roughly 1310 Newtons, which is not enough to over power the 1400 Newtons of the projected frictional braking performance of the braking system. As a result, our primitive test's results aligns with our physical analysis of the braking system and as such verifies the braking performance of the pod to the best of our ability without being able to engage the on board motors.

#### Compare results to initial performance requirements

Our initial performance requirements maintained that we were going to attain a braking deceleration of greater than 2 g's. This performance metric is measured by the braking force divided by the pod mass. Therefore, our braking deceleration is estimated to be around 2.2 g's of braking force assuming a 60 kilogram pod mass. This exceeds our initial goal of 2 g's and is the

highest deceleration braking system in the team's history. In addition to this, the HyperXite VII braking system is the first HyperXite braking system to feature fail-safe behavior since HyperXite IV. Following this, many more improvements have been made over previous years of braking.

Photos with Annotations

## Description of Final Design

### Document prototype development and redesign

The braking system has been designed iteratively throughout the course of the academic year. While initially we started with two major designs; the web and flange designs, after the first 10 weeks we shifted gears towards emphasizing the perpendicular flange design. From then on we determined the best avenue for improvement over the previous years braking design was to scale up in a cost conscious manner. To do so we catalogued the hardware we already had in our reserves in order to design around reusing existing hardware as a design constraint. We determined it would be most effective to utilize an 8 actuator design as opposed to the 4 actuator design of HyperXite VI. Over the course of the winter quarter, we focused on implementing gas springs in order to maintain braking force during a pod fault. This process consisted of determining an effective gas spring to integrate emphasizing the importance of both size and actuation force. We settled on the McMaster 6643K62 Miniature Gas Spring, and after selecting it the majority of design decisions were influenced by this specific part. The finer design considerations are discussed in Chapter 3 Critical Design.

Lastly during the Spring Quarter, we shifted greatly towards the manufacturing of our design, we finished creating the Braking Test Rig that was initially designed during HyperXite VI, and attempted to collect experimental data that we could use to quantify the improvements of our braking systems through the years; however, unfortunately we were unable to collect meaningful data because of electrical failures in the braking test rig's Electronic Speed Controller. Finally, we finished the final version of the braking system by the end of May ready to be integrated into the pod as whole.

Our braking system is best characterized as a Fail-Closed pneumatically actuated frictional braking system and is depicted in the following images:



*Figure 22 - Pod After Assembly in Lab*



*Figure 23 - Pod on I-Beam During Pod Runs*

Finalized Engineering drawings



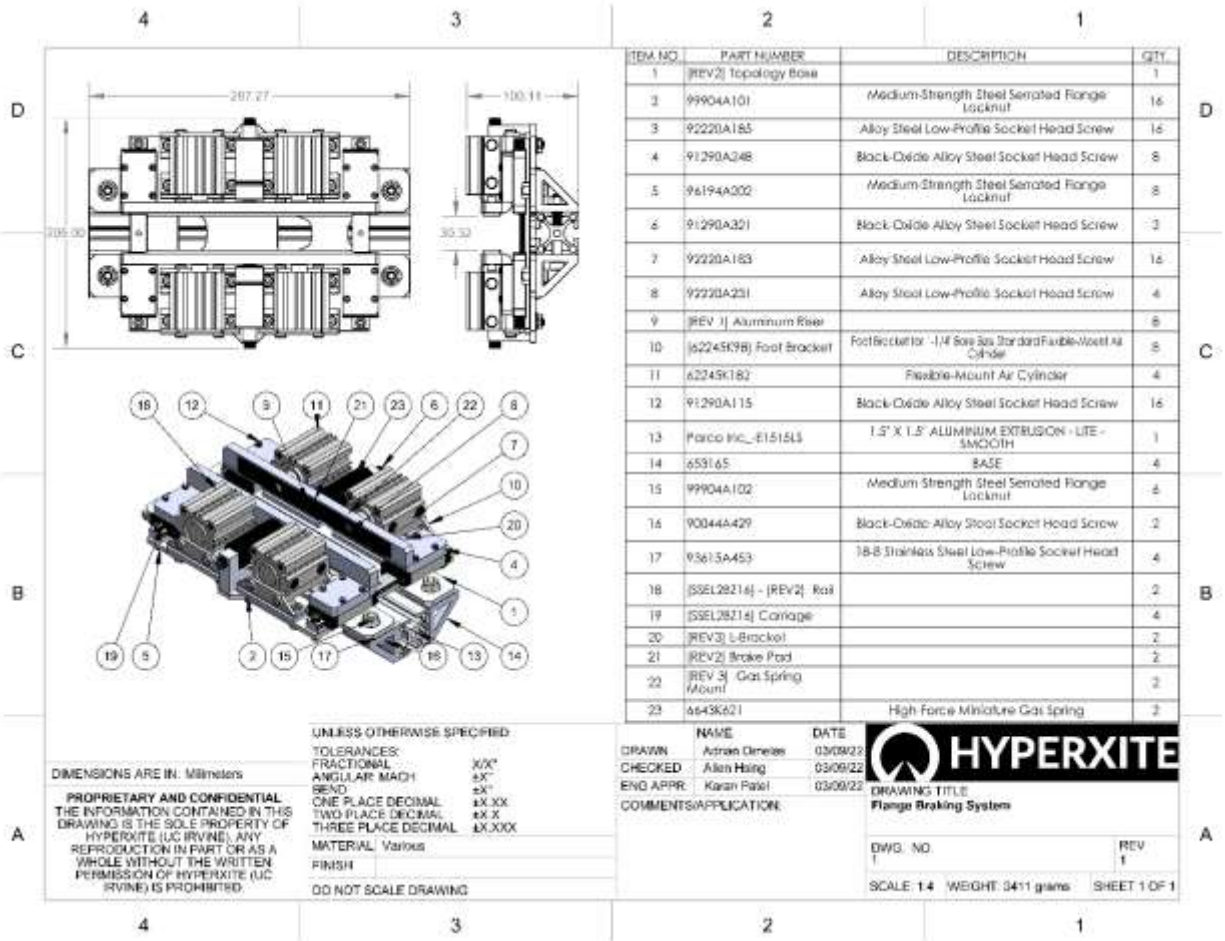


Figure 24 - Final Engineering Drawing

### Finalized Bill of Materials

ITEM NO.	PART NUMBER	DESCRIPTION	QTY USED Per Braking System	QTY TOTAL	Orders to Place	Amount per Order	Price	Exhaustive Price	Need to Order	Supplier
101	99904A1	Medium-Strength Steel Serrated	16	32	1	100	\$6.90	\$6.90	\$6.90	McMaster-Carr

		Flange Locknut									
2	85	Alloy Steel Low- Profile Socket Head Screw	16	32	1	50	\$11.84	\$11.84	\$11.84	McMaster -Carr	
3	48	Black- Oxide Alloy Steel Socket Head Screw	8	16	1	50	\$11.06	\$11.06	\$11.06	McMaster -Carr	
4	02	Medium- Strength Steel Serrated Flange Locknut	8	16	1	100	\$8.86	\$8.86	\$8.86	McMaster -Carr	
5	21	Black- Oxide Alloy Steel Socket Head Screw	2	4	1	100	\$15.14	\$15.14	\$15.14	McMaster -Carr	
6	83	Alloy Steel Low- Profile Socket Head Screw	16	32	0	50	\$11.85	\$0.00	\$0.00	McMaster -Carr	

7	31	Alloy Steel Low- Profile Socket Head Screw	4	8	1	5	\$6.65	\$6.65	\$6.65	McMaster -Carr
8	8	Foot Bracket for 1-1/4" Air Cylinder	8	16	16	1	\$8.07	\$129.12	\$129.12	McMaster -Carr
9	82	Flexible- Mount Air Cylinder	4	8	8	1	\$61.66	\$493.28	\$493.28	McMaster -Carr
10	5	Black- Oxide Alloy Steel Socket Head Screw	16	32	1	100	\$9.08	\$9.08	\$9.08	McMaster -Carr
11	E1515LS	1.5" X 1.5" ALUMINU M EXTRUSIO N -11.5 Inches	1	2	2	1	\$6.58	\$13.16	\$13.16	parco- inc
12	653165	CG322H Corner Gusset	4	8	8	1	\$6.10	\$48.80	\$48.80	framinge tech
13	02	Medium- Strength Steel	6	12	1	100	\$10.34	\$10.34	\$10.34	McMaster -Carr



		Serrated Flange Locknut									
14	29	90044A4 Black- Oxide Alloy Steel Socket Head Screw	2	4	1	10	\$12.8 3	\$12.83	\$12.83	McMaster -Carr	
15	53	93615A4 18-8 Stainless Steel Low- Profile Socket Head Screw	4	8	2	5	\$5.24	\$10.48	\$10.48	McMaster -Carr	
16	6	SSEL2BZ1 High Strength Linear Rail + 2 Carriages	2	4	4	1	\$127. 66	\$510.64	\$510.6 4	Misumi	
17	1	6643K62 High- Force Miniature Gas Spring	2	4	4	1	\$88.69	\$354.76	\$354. 76	McMaster -Carr	

Table 2 - Finalized Bill of Materials

### Detailed Cost Analysis

Trough careful consideration of our existing project inventory we were able to minimize the cost of the braking system. Instead of buying new actuators, we were able to reincorporate all 4 actuators from the previous year's braking system, and an additional 4 that we had in reserve. Unfortunately, due to a manufacturing miscommunication with our laser cutting contractor,

SendCutSend, our Braking main bracket that was used to transfer the force from our actuators and springs to our frictional brake pads was manufactured at only 80% of the thickness. This error resulted in our braking bracket to fail the factory of safety and we had to redesign this part from 5052 Aluminum to 4130 Chromoly Steel last minute during the final weeks of the project.

**Safety and Risk Assessment**

**FMEA:**

Item	Failure Mode	Failure Effects	SEV	Causes	OCC	Controls	DET	RISK
Linear Rails	Bending moment	Carriages shear off Linear rail and L-bracket falls off	7	Large normal force which leads to large braking force	1	Gas spring mount defines braking force which will not allow braking force to cause this failure mode	1	7
	Collision with I-beam	Carriages shear off Linear rail and L-bracket falls off Restriction of motion	7	Braking system mounted to close to I-beam	1	Braking system is mounted clear of the no-go zone and dynamics systems prevents lateral displacement	2	14
Gas Spring	Dirt or other Contaminate	Progressive damage loss of braking force	4	Improper storage of gas spring	1	Gas spring is stored in a clean environment	3	12
	Loss of Pressure	Loss of the high pressure nitrogen gas therefore loss of braking force	6	Seal becomes damaged	3	Gas spring is handled with care and inspected prior to use	2	36
L-Bracket	Stress Failure	Loss of contact force with I-beam	8	Large normal force which leads to large braking force	2	Gas spring mount defines braking force which will not allow braking force to cause this failure mode	1	16

Brake Pad	Thermal Failure	Brake pad melts and causes I-beam damage	5	Repeated braking without breaks in between	2	Braking run is defined as having one actuation per run and must have a 10 minute break in between for cooling	1	10
	Adhesive Failure	Brake pad disconnects from L-bracket	7	Epoxy not cured properly or large shear force	1	Epoxy is applied by fully curing for 24 hours	2	14
Foot Bracket	Stress Failure	Loss of pneumatic actuator restrictive force (Forced Braking Condition)	3	Bolts holding foot bracket shears off	2	Gas spring mount defines braking force which will not allow braking force to cause this failure mode	1	6
Gas Spring Mount	Stress Failure	Loss of braking force	6	Large normal force which leads to large braking force	3	Gas spring mount defines braking force which will not allow braking force to cause this failure mode	1	18
Integration with Aluminum Extrusion	Detachment from Chassis	Braking assembly slides off of braking	8	Large shearing force causes screws to shear off	1	Gas spring mount defines braking force which will not allow braking force to cause this failure mode	4	32

Table 3 - FMEA

## Chapter 5: Design Recommendations and Conclusions

### **Summarize accomplishments:**

The accomplishments of the UCI HyperXite Braking team can be grouped into three different categories: designing, manufacturing, and testing. During fall quarter the braking design with a failsafe was finalized as well as the integration of the braking system to the chassis. As a part of our design process, we validated the design using ANSYS to confirm that none of the components will fail under the expected loads of the braking force. During winter quarter, we began the manufacturing process. We confirmed the needed off the shelf components to manufacture the braking system. During this time, we also manufactured the braking test rig. By the end of winter quarter, the braking system was assembled as well as the braking test rig. The braking test rig was functional using the rotary encoder, Odrive, and thermal sensor. During spring quarter, we began testing the braking test rig and collecting data such as the braking distance, braking time, and temperature. Finally, we integrated the braking system to the chassis.

### **Design recommendations for the future:**

In the future, one design change could be implemented to further improve the design of the braking system. Firstly, the braking force can be further maximized by using different actuators. The EHW limits how much pressure the actuators can exert based on the maximum allowable pressure of the actuator by enforcing a factor of safety of 2. By using heavier duty actuators, the braking force achieved can be up to 3G's. This will allow the pod to travel to even higher speeds.

### **Lessons learned:**

Prioritizing time and having a clear engineering process can help to keep the project on track and avoid delays. The nature of senior design projects is very time sensitive. Prioritizing and utilizing the time we have during the year is very important. While we were efficient in our process sometimes getting stuck in an iterative loop can waste time and delay timelines. Having team members focus on specific tasks can help the team be more efficient as well.

### **Conclusions:**

Overall, the HyperXite braking team has designed and developed a braking system that can exert 2G's of braking force to bring the pod to a stop. The parts of the system have been validated on ANSYS and the overall braking system has been validated using the braking test rig and the with pod runs. The failsafe will provide a second layer of redundancy to the braking system so in case of a pneumatic failure, the braking system can still exert a braking force on the pod.

## Acknowledgements

We want to express our greatest thanks to the HyperXite VII team, from every sub team, to our confident management, every single person helped make this team shine bright like a star!

We want to thank Professor Roger Rangel for always supporting us and allowing us to thrive as a team. (MAE Chair, rhrangel@uci.edu

We would like to thank this year's HyperXite sponsors: The Green Initiative Fund (TGIF), UROP, Intellian Technologies Inc., Northrop Grumman, Nord-Lock Group, Rockwell Automation, and ANSYS. We are exceptionally grateful for their support because they enable us to keep pushing boundaries.

## References

Tsuchiya, Masa. "NB Corporation | Linear Motion System Life Resource | Nippon Bearing." NB Corporation, [www.nbcorporation.com/engineering-info/life/](http://www.nbcorporation.com/engineering-info/life/). Accessed 11 June 2022.

"HUMAN PERFORMANCE CAPABILITIES." Msis.jsc.nasa.gov, [msis.jsc.nasa.gov/sections/section04.htm#Figure%204.9.3-6](http://msis.jsc.nasa.gov/sections/section04.htm#Figure%204.9.3-6).

# Appendix

## Assembly Documentation

### Braking General Assembly Instructions

<b>Reference Assignments</b>	38
<b>Required Tools</b>	41
<b>Assembly</b>	41
Base Plate Preparation and Mounts	42
Gas Spring Mount Installation	42
Air Cylinder Foot Bracket Installation	44
Linear Rail Installation	45
Actuators and Brackets	47
Air Cylinders	48
Braking L-Brackets	48
Gas Springs	49
Mounting Solution	52
Mounting Solution	52
Reference Assignments	

Qt.	Ref #	Image	Part Name
1	1A		Braking Base Plate
2	1B		Gas Spring Mount
8	1C		[91290A248] Black-Oxide Alloy Steel Socket Head Screw
8	1D		[96194A202] Medium-Strength Steel Serrated Flange Locknut

8	1E		Aluminum Riser
8	1F		[62245K98] Foot Bracket
16	1G		[92220A185] Alloy Steel Low-Profile Socket Head Screw
16	1H		[99904A101] Serrated Flange Locknut
4	1I		[SSEL2BZ16] Carriage
2	1J		[SSEL2BZ16] - Linear Rail
4	2A		[62245K182] Air Cylinder
16	2B		[62245K98] Air Cylinder Foot Bracket Included Fasteners

2 2C



Braking L-Bracket

16 2D



[91290A115] Black-Oxide Alloy Steel Socket Head Screw

4 2E



[92220A231] Low-Profile Socket Head Screw

2 2E



[6643K621] High-Force Miniature Gas Spring

2 2F



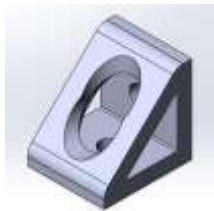
[91290A321] Black-Oxide Alloy Steel Socket Head Screw

1 3A



11.3 Inch Aluminum Extrusion

4 3B



[CG322H] Corner Gusset

6 3C



[99904A102] Medium-Strength Steel Serrated Flange Locknut



4 3D



[93615A453] 18-8 Stainless Steel Low-Profile Socket Head Screw

2 3E



[90044A429] Black-Oxide Alloy Steel Socket Head Screw

#### Required Tools

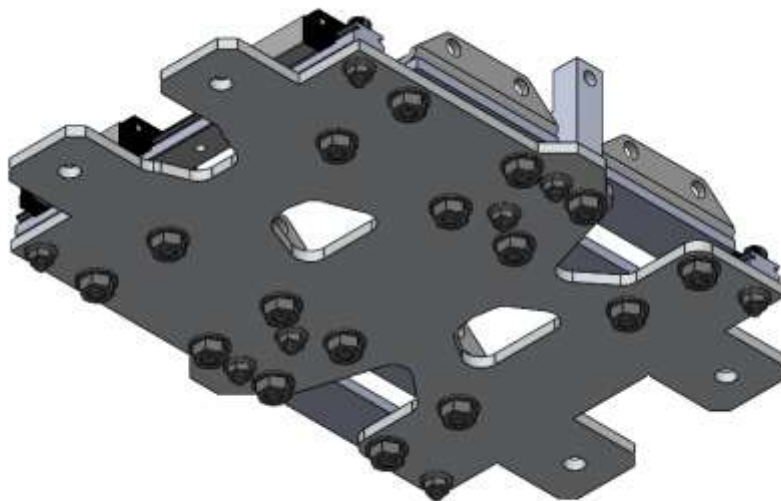
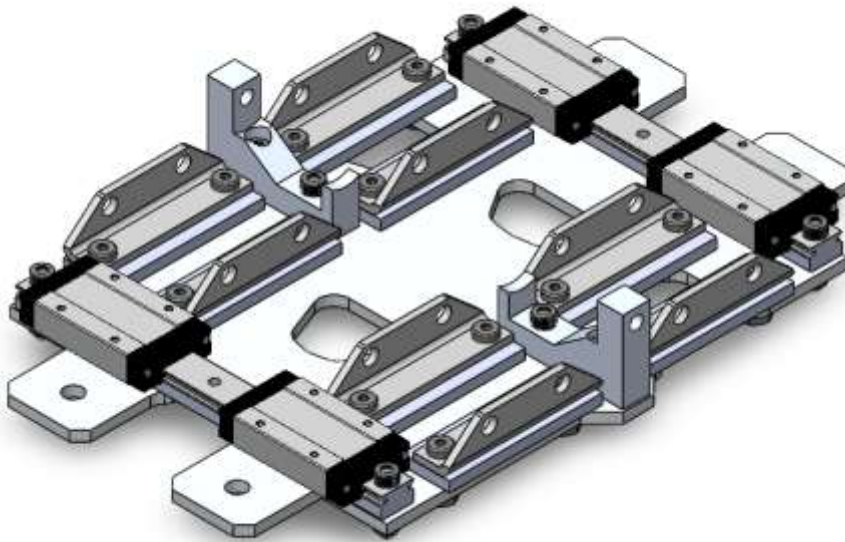
##### Hex Keys:

- 2.5 mm
- 4 mm
- 5 mm
- 1/8 Inch
- 1/4 Inch
- 5/32 Inch
- One Unknown Imperial Hex Key (Will be corrected)

##### Sockets (Alternatively one wrench)

- 8 mm
- 7/16th Inch
- 1/2 Inch

Assembly  
Base Plate Preparation and Mounts  
Final Images of **Base Plate Preparation and Mounts**



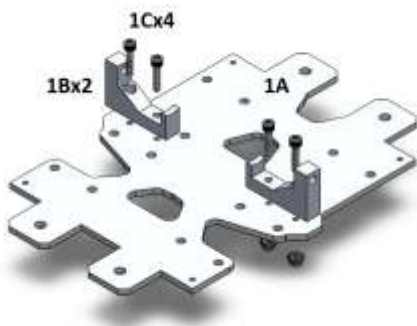
Gas Spring Mount Installation

NOTES: Also includes first mount on Base Plate

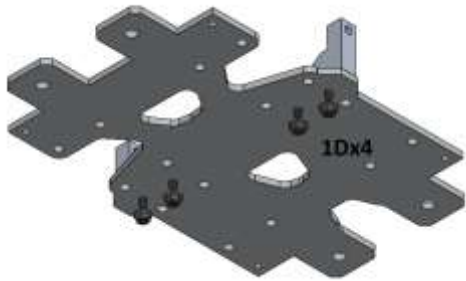
Tools: 4 mm Hex Key, 8 mm Hex Socket / Wrench

Utilizes:

Qt.	Ref #	Image	Part Name
1	1A		Braking Base Plate
2	1B		Gas Spring Mount
4	1C		[91290A248] Black-Oxide Alloy Steel Socket Head Screw
4	1D		[96194A202] Medium-Strength Steel Serrated Flange Locknut



Align Gas Spring Mounts (1B) with lower flanges facing each other onto the Braking Base Plate (1A) and fasten with [91290A248] Black-Oxide Alloy Steel Socket Head Screw (1C).



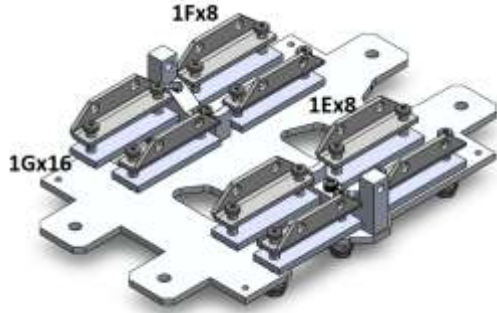
Fasten each screw to the corresponding [96194A202] Serrated Flange Locknut (1D) with a combination of hex socket / wrench and hex key until secure. Locknut should deform the aluminum plate slightly to “Lock” in place.

### Air Cylinder Foot Bracket Installation

Tools: 1/8 Inch Hex Key, 7/16 Inch Hex Socket / Wrench

Utilizes:

Qt.	Ref #	Image	Part Name
8	1E		Aluminum Riser
8	1F		[62245K98] Foot Bracket
16	1G		[92220A185] Alloy Steel Low-Profile Socket Head Screw
16	1H		[99904A101] Serrated Flange Locknut



Similar to before, align Aluminum Risers (1E) and [62245K98] Foot Bracket (1F) with flanges opposite each other like so in the image. (The upper flange of the edge foot bracket should be raised on the edge size) The Aluminum riser is symmetrical and not dependent on orientation. Once aligned correctly, thread [92220A185] Alloy Steel Low-Profile Socket Head Screw (1G) through the two holes to keep concentric.



Finally, fasten each of the 16 screws to the corresponding [99904A101] Serrated Flange Locknut (1H) with a combination of hex socket / wrench and hex key until secure. Locknut should deform the aluminum plate slightly to “Lock” in place.

#### Linear Rail Installation

Tools: 4 mm Hex Key, 8 mm Hex Socket / Wrench

Utilizes:

Qt.	Ref #	Image	Part Name
4	1I		[SSEL2BZ16] Carriage
2	1J		[SSEL2BZ16] - Linear Rail

4 1C

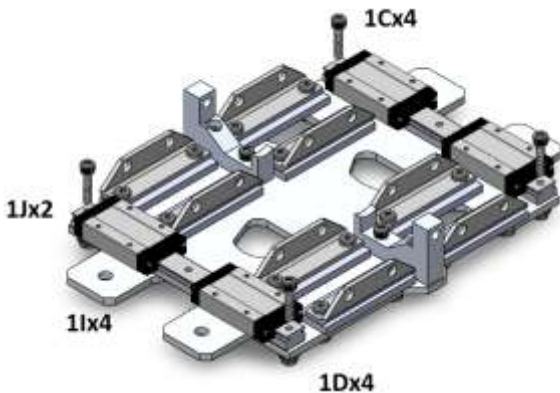


[91290A248] Black-Oxide Alloy Steel Socket Head Screw

4 1D

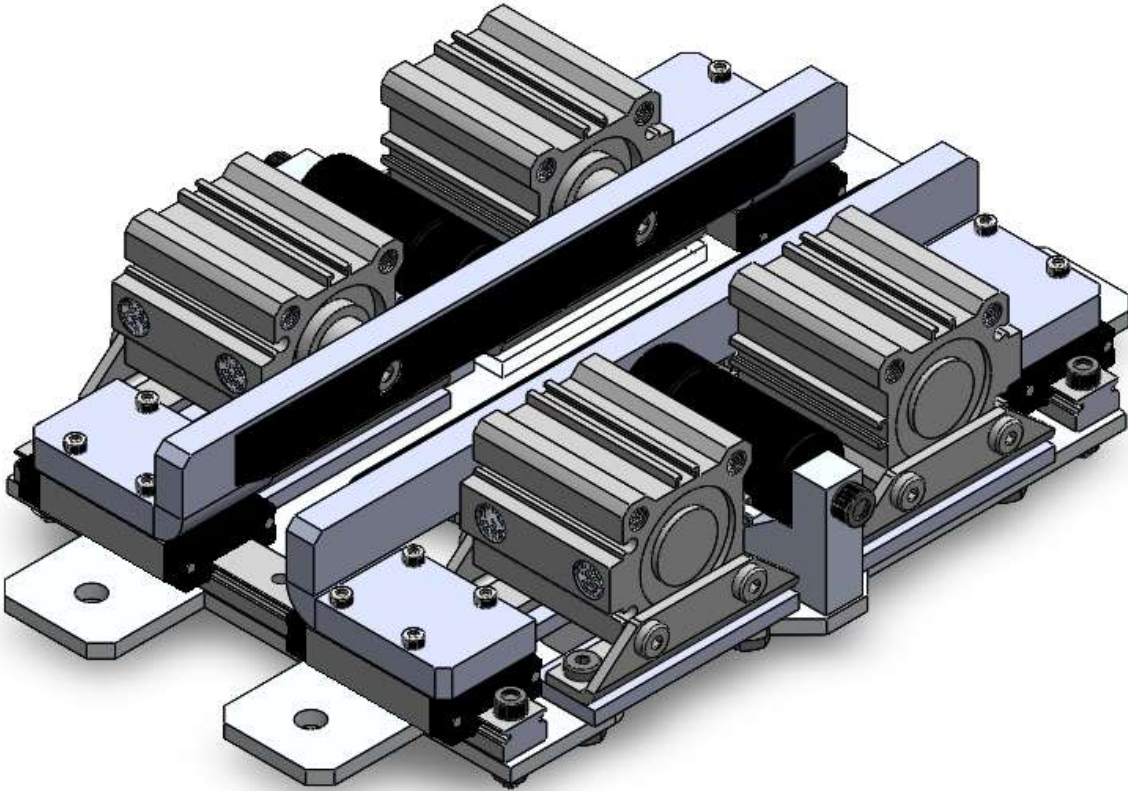


[96194A202] Medium-Strength Steel Serrated Flange Locknut



Before fastening linear rail to braking base plate, **ensure that carriages are mounted onto the linear rail.** It is impossible to slide carriages on after linear rail is fastened. Fasten the two linear rails similarly to before using the combination of [91290A248] Black-Oxide Alloy Steel Socket Head Screw (1C) and [96194A202] Medium-Strength Steel Serrated Flange Locknut (1D) used before.

Actuators and Brackets  
Final Image of Actuators and Brackets



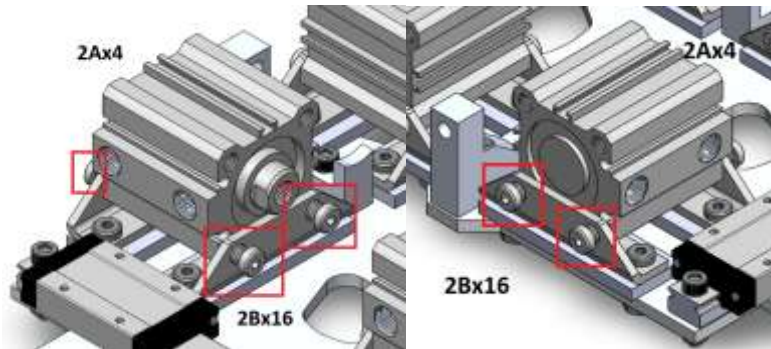


## Air Cylinders

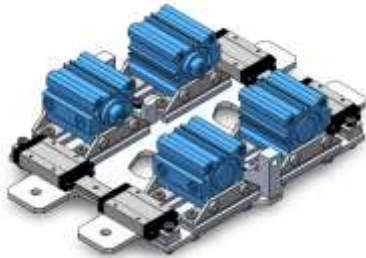
Tools: Unknown Imperial Hex Key

Utilizes:

Qt.	Ref #	Image	Part Name
4	2A		[62245K182] Air Cylinder
16	2B		[62245K98] Air Cylinder Foot Bracket Included Fasteners



Use the included foot bracket fasteners (2B, boxed in red) to secure the [62245K182] Air Cylinder (2A) to the foot brackets. **Please ensure that the pneumatic fitting on each air cylinder faces the nearest carriage to aid with routing the pneumatic plastic pipes.**



Repeat process for all 4 pneumatic air cylinders.

Braking L-Brackets

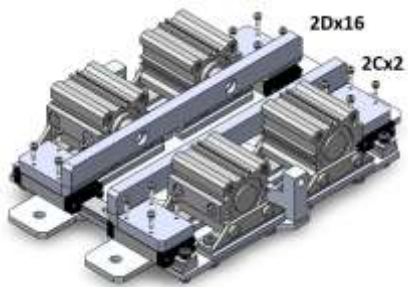
NOTE: Bracket is shown without Brake Pad material



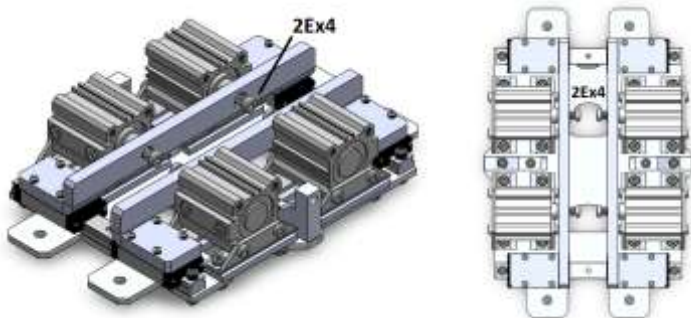
Tools: 5/32 Inch and 2.5 mm Hex Key

Utilizes:

Qt.	Ref #	Image	Part Name
2	2C		Braking L-Bracket
16	2D		[91290A115] Black-Oxide Alloy Steel Socket Head Screw
4	2E		[92220A231] Low-Profile Socket Head Screw



Align Braking L-Bracket (2C) with carriages on Linear Rails and fasten down with 16 [91290A115] Black-Oxide Alloy Steel Socket Head Screws (2D) and a 2.5mm Hex Key.





Once Bracket is secured to carriages, move bracket flush to Air Cylinders and fasten Bracket (2C) to Air Cylinders (2A) with 4 [92220A231] Low-Profile Socket Head Screws (2E) and 5/32th Inch Hex Key.

Gas Springs

**Warning: The Miniature Gas Spring can store 173 lbs of force, be careful!**

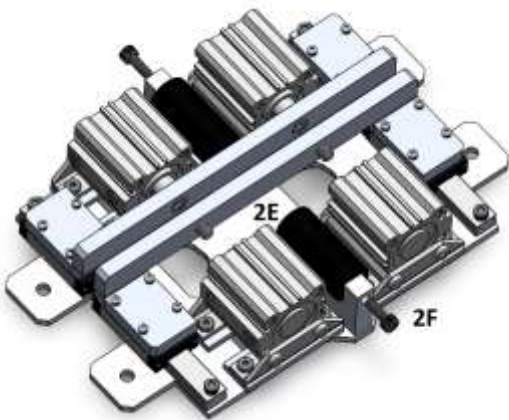
Tools: 5 mm Hex Key, Clamps?

Utilizes:

Qt.	Ref #	Image	Part Name
2	2E		[6643K621] High-Force Miniature Gas Spring
2	2F		[91290A321] Black-Oxide Alloy Steel Socket Head Screw

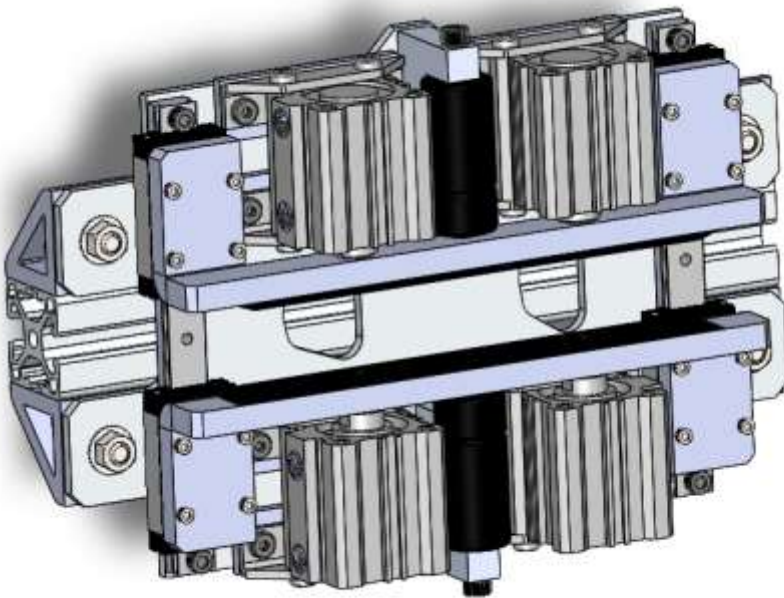
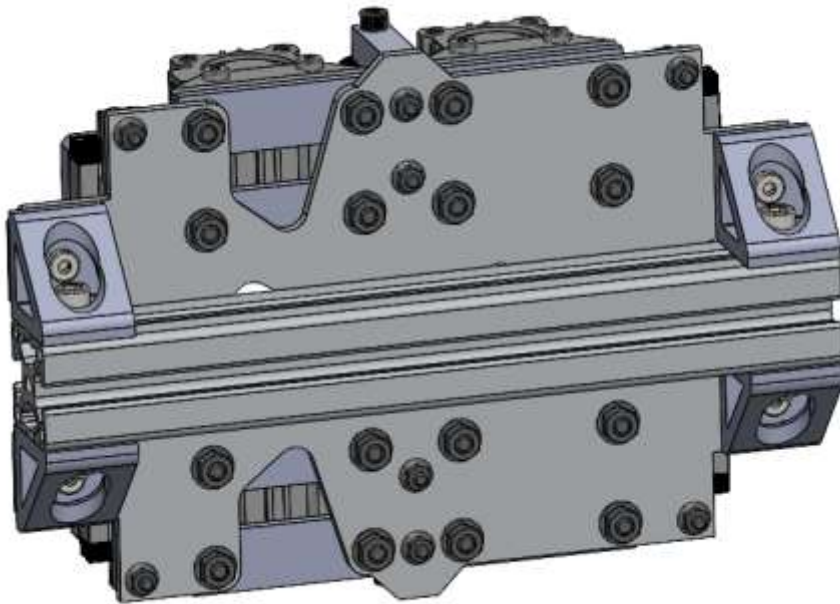


With the bracket free to move, fully extend one side of the actuators and screw in the [6643K621] High-Force Miniature Gas Spring (2E) with a [91290A321] Black-Oxide Alloy Steel Socket Head Screw (2F) in the created gap.



Similarly on the other side, repeat the process. However, now that one gas spring is installed, the opposite braking L-Bracket (2C) will have to be restrained by a clamp or some other restrictive force (possibly the pneumatic actuators themselves if the pneumatic base station is ready).

Mounting Solution  
Final Images of **Mounting Solution**

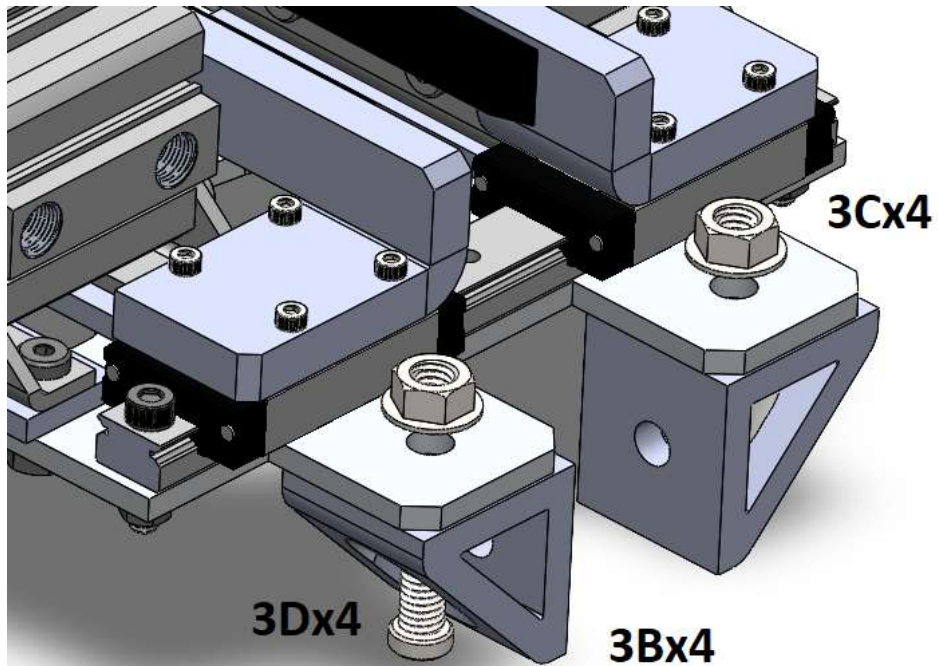


Mounting Solution

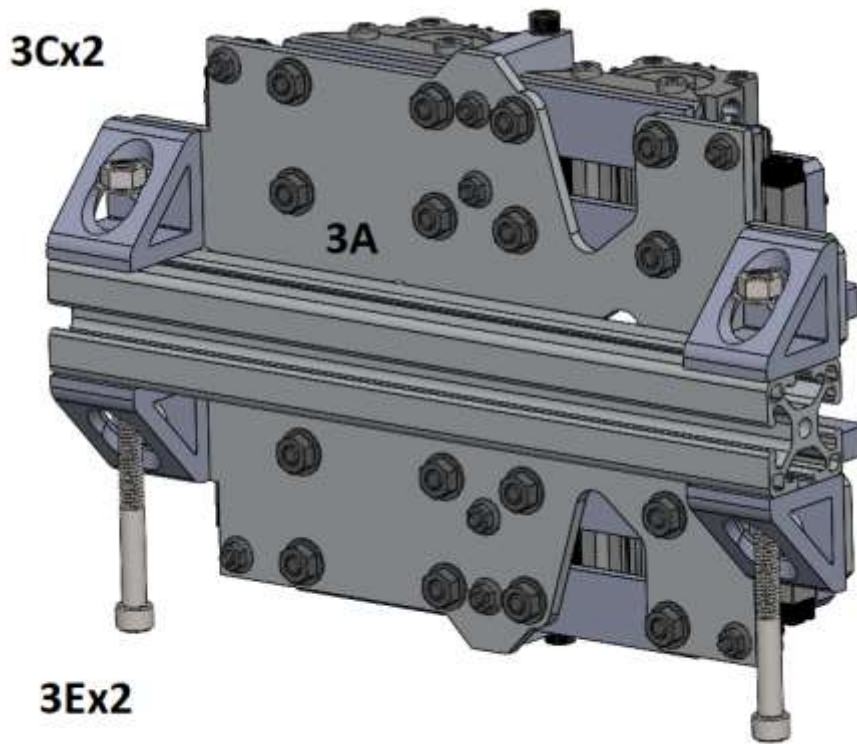
Tools: 5/32 Inch Hex Key, 1/4 Inch Hex Key, 1/2 Inch Hex Socket/Wrench

Utilizes:

Qt.	Ref #	Image	Part Name
1	3A		11.3 Inch Aluminum Extrusion
4	3B		[CG322H] Corner Gusset
6	3C		[99904A102] Medium-Strength Steel Serrated Flange Locknut
4	3D		[93615A453] 18-8 Stainless Steel Low-Profile Socket Head Screw
2	3E		[90044A429] Black-Oxide Alloy Steel Socket Head Screw



Fasten all four [CG322H] Corner Gussets (3B) to each of the “Ears” of the Braking Base Plate (1A) using the combination of [99904A102] Medium-Strength Steel Serrated Flange Locknuts (3C) and [93615A453] 18-8 Stainless Steel Low-Profile Socket Head Screws (3D). Make sure that the flat flange faces the inside of the braking base plate to fasten onto the Aluminum Extrusion (3A).



Once the Aluminum Extrusion is fitted between the [CG322H] Corner Gussets (3B), secure it using a combination of [99904A102] Medium-Strength Steel Serrated Flange Locknuts (3C) and [90044A429] Black-Oxide Alloy Steel Socket Head Screws (3E).

